Nuclear magnetic octupole moment and the hyperfine structure of the $5D_{3/2,5/2}$ states of the Ba$^+$ ion

K. Beloy,[1] A. Derevianko,[1, 2] V. A. Dzuba,[2] G. T. Howell,[3] B. B. Blinov,[3] and E. N. Fortson[3]

[1] *Physics Department, University of Nevada, Reno, Nevada 89557*

[2] *School of Physics, University of New South Wales, Sydney 2052, Australia*

[3] *Department of Physics, University of Washington, Seattle, Washington 98195*

(Dated: April 28, 2008)

Abstract

The hyperfine structure of the long-lived $5D_{3/2}$ and $5D_{5/2}$ levels of Ba$^+$ ion is analyzed. A procedure for extracting relatively unexplored nuclear magnetic moments Ω is presented. The relevant electronic matrix elements are computed in the framework of the *ab initio* relativistic many-body perturbation theory. Both the first- and the second-order (in the hyperfine interaction) corrections to the energy levels are analyzed. It is shown that a simultaneous measurement of the hyperfine structure of the entire $5D_J$ fine-structure manifold allows one to extract Ω without contamination from the second-order corrections. Measurements to the required accuracy should be possible with a single trapped barium ion using sensitive techniques already demonstrated in Ba$^+$ experiments.

PACS numbers: 32.10.Fn,31.15.am,21.10.Ky,27.60.+j

1

I.   INTRODUCTION

A nucleus as a source of the electro-magnetic fields is conventionally described using a hierarchy of static electromagnetic moments: magnetic dipole (M1,μ), electric quadrupole (E2, Q), magnetic octupole (M3,Ω), etc. Interaction of atomic electrons with these moments leads to the hyperfine structure (HFS) of the atomic energy levels. While the first two moments, μ and Q, have been studied extensively, the octupole moments remain relatively unexplored.

While octupole moments may be approximated using the nuclear-shell model [1], the correct values depend strongly on nuclear many-body effects and, in particular, on core-polarization mediated by the nucleon spin-spin interaction [2]. Senkov and Dmitriev [2] carried out a nuclear-structure calculation of Ω for ^{209}Bi. In this particular case, the polarization effects enhance the shell-model values by a factor of three. According to Dmitriev [3], a systematic study of octupole moments will help place constraints on the poorly-known isoscalar part of nuclear spin-spin forces. In another, even more striking example, the deduced value of Ω of ^{133}Cs is forty times larger than the shell-model value [4] (this has not been analyzed yet in nuclear theory). We note that in the case of Cs, the shell-model value is strongly suppressed due to an accidental cancellation between the orbital and spin contributions of the valence proton to the magnetic-octupole moment.

Measuring the effects of the octupole moments on the hyperfine structure was so far limited to a small number of atoms: Cl [5], Ga [6], Br [7], In [8], V [9], Eu [10], Lu [11], Hf [12], and Bi [13]. Since deducing Ω from a measurement requires knowing atomic-structure couplings, previous analysis focused primarily on *isotopic ratios* because the electronic coupling factor cancels out when ratios of HFS constants are formed. An exception is the measurement on the $6P_{3/2}$ state of ^{133}Cs [4], where sufficiently accurate calculations are possible. In a recent paper [14], we argued that an accurate deduction of the octupole moments is feasible for metastable $^3P_2$ states of alkaline-earth atoms.

Ba$^+$, being an atomic system with one valence electron outside a closed-shell core, also presents a case where both high-accuracy measurements and high-accuracy calculations are possible. The goal of this paper is to analyze the hyperfine structure of the $5D_{3/2}$ and $5D_{5/2}$ levels of Ba$^+$, and to show that Ba$^+$ is a particularly favorable case for measuring octupole moments, for both theoretical and experimental reasons. Both $5D$ levels belong

to the same fine-structure manifold. We take advantage of a simultaneous analysis of the hyperfine structure of both levels and show that such an analysis allows to eliminate the potentially troublesome second-order hyperfine electron structure term thus providing a powerful consistency test for the measurements and calculations and possibly improving the accuracy of deducting Ω. Furthermore, $5D_{3/2}$ and $5D_{5/2}$ are each long lived metastable states in Ba$^+$, with lifetimes of about 80s and 30s respectively. Hyperfine intervals thus could be measured in principle to well below 0.1Hz, much better than in previous octupole experiments; techniques to exploit the sensitivity inherent in the 5D levels have already been developed using single trapped Ba$^+$ [15].

Barium has two stable odd isotopes, 135 and 137. Both isotopes possess nuclear ground states with spin of $I = 3/2$ and of positive parity. The values of the magnetic and quadrupole moments are

$$^{135}\text{Ba} : \mu = 0.837943\,\mu_N\,, Q = +0.160\,\text{b}\,,$$

$$^{137}\text{Ba} : \mu = 0.937365\,\mu_N\,, Q = +0.245\,\text{b}\,, \tag{1}$$

where μ_N is the nuclear magneton and b (barn) $= 10^{-24}$ cm^2. Both isotopes have unpaired neutrons in the $d_{3/2}$ single-particle state, and from the single-particle (shell) model [1] we may estimate the octupole moment to be

$$\Omega^{\text{sp}} = 0.164\mu_N\langle r^2\rangle \approx 0.0385\,\mu_N \times \text{b}\,, \tag{2}$$

where we used the rms value of the nuclear radius $\langle r^2\rangle^{1/2} = 4.84\,\text{fm}$. Of course, the shell model is only an approximation. For example, in contrast to the known properties (1) for the two isotopes, this model would produce identical values of the magnetic moments and vanishing values of the quadrupole moments.

This paper is organized as follows. First we recapitulate the theory of the hyperfine structure of atomic levels, including octupole moments and the second-order effects. We present specific formulae for the Ba case and show how to extract the octupole constant C from hyperfine intervals (to be measured). Further we compute the electronic structure factor required for extracting the octupole moment from the constant C. Finally, we present a brief description of an experimental method with single Ba$^+$ to determine the octupole moments of ^{135}Ba and ^{137}Ba. We follow the notation and formalism of the recent paper [14]. Unless specified otherwise, atomic units, $\hbar = |e| = m_e = 1$, and Gaussian electromagnetic units are employed throughout.

II. PROBLEM SETUP

Hyperfine-interaction (HFI) Hamiltonian, describing coupling of electrons to various nuclear moments may be represented in the tensorial form of

$$H_{\mathrm{HFI}} = \sum_{k,q} (-1)^q \, T^e_{k,q} T^n_{k,-q}.$$

Here the spherical tensors (of rank k) $T^e_{k,q}$ act on the electronic coordinates. Tensor operators $T^n_{k,q}$ are the components of the nuclear electric and magnetic 2^k-pole (MJ and EJ; T,P-even) moment operators. In particular, the conventionally-defined magnetic-dipole, electric-quadrupole, and magnetic-octupole moments of the nucleus are proportional to the expectation values of the zero-component ($q = 0$) operators in the nuclear stretched states $|I, M_I = I\rangle$: $\mu = \langle T^n_{k=1}\rangle_I$, $Q = 2\langle T^n_{k=2}\rangle_I$, and $\Omega = -\langle T^n_{k=3}\rangle_I$. Explicit expressions for the electronic operators and the corresponding reduced matrix elements are tabulated in Ref. [14].

The conserved angular momentum $\mathbf{F}$ for the hyperfine coupling is composed from atomic, $\mathbf{J}$, and nuclear, $\mathbf{I}$, angular momenta: $\mathbf{F} = \mathbf{I} + \mathbf{J}$. It is convenient to work in a basis spanned by the eigenfunctions $|\gamma I J F M_F\rangle$ which is formed by coupling atomic, $|\gamma J M_J\rangle$, and nuclear, $|I M_I\rangle$, wave functions. Here γ encapsulates remaining electronic quantum numbers. For $I = 3/2$ each of the $5D_J$ levels splits into four hyperfine components: $5D_{3/2}$ has hyperfine components $F = 0, 1, 2, 3$, and $5D_{5/2}$ has components $F = 1, 2, 3, 4$.

Owing to the HFI's rotational invariance, a matrix element of the HFI in the $|\gamma I J F M_F\rangle$ basis is diagonal in the quantum numbers F and M_F. If we limit our system of levels to only the $5D_J$ fine-structure manifold, the hyperfine components $F = 1, 2, 3$ of the $5D_{3/2}$ and $5D_{5/2}$ levels become coupled. The intervals within each manifold may be parameterized using the conventional hyperfine constants A, B, C and the second-order corrections (in HFI) η and ζ. Constants A, B, C are proportional to nuclear moments μ, Q, and Ω. M1-M1 correction η is of the second order in μ, and ζ comes from a cross-term between M1 and E2 parts of the HFI. Second-order corrections are suppressed by a large energy denominator equal to the fine-structure splitting between the $5D_J$ levels.

The energy intervals $\delta W^{(J)}_F = W^{(J)}_F - W^{(J)}_{F+1}$ within each fine-structure manifold $5D_J$ are

as follows. For $5D_{3/2}$,

$$\delta W_0^{(3/2)} = -A + B - 56C + \frac{1}{100}\eta - \frac{1}{100}\sqrt{\frac{7}{3}}\zeta,$$

$$\delta W_1^{(3/2)} = -2A + B + 28C + \frac{1}{75}\eta,$$

$$\delta W_2^{(3/2)} = -3A - B - 8C + \frac{1}{300}\eta + \frac{1}{20}\sqrt{\frac{3}{7}}\zeta, \tag{3}$$

and for $5D_{5/2}$,

$$\delta W_1^{(5/2)} = -2A + \frac{4}{5}B - \frac{96}{5}C - \frac{1}{75}\eta,$$

$$\delta W_2^{(5/2)} = -3A + \frac{9}{20}B + \frac{81}{5}C - \frac{1}{300}\eta - \frac{1}{20}\sqrt{\frac{3}{7}}\zeta,$$

$$\delta W_3^{(5/2)} = -4A - \frac{4}{5}B - \frac{32}{5}C + \frac{2}{75}\eta + \frac{2}{25\sqrt{21}}\zeta. \tag{4}$$

In the above equations the HFS constants A, B, and C are all specific to the state of consideration while η and ζ represent the same second-order HFS constant.

If we assume all other second- and higher-order effects are negligible (see justification in Section IV), then we may solve for the HFS constants A, B, and C in terms of the HFS intervals and these two second-order constants. Specifically, solving for the C constants:

$$C(5D_{3/2}) = -\frac{1}{80}\delta W_0^{(3/2)} + \frac{1}{100}\delta W_1^{(3/2)} - \frac{1}{400}\delta W_2^{(3/2)} - \frac{1}{2000\sqrt{21}}\zeta,$$

$$C(5D_{5/2}) = -\frac{1}{40}\delta W_1^{(5/2)} + \frac{1}{35}\delta W_2^{(5/2)} - \frac{1}{112}\delta W_3^{(5/2)} + \frac{1}{200\sqrt{21}}\zeta. \tag{5}$$

The C constants do not depend on the M1-M1 η correction, as was proven in Ref. [14] on general grounds.

It is possible to use Eqs. (5) to cancel the constant ζ and therefore eliminate the second-order effects from the problem altogether. In doing so, we obtain the equation

$$C(5D_{3/2}) + \frac{1}{10}C(5D_{5/2}) = -\frac{1}{80}\delta W_0^{(3/2)} + \frac{1}{100}\delta W_1^{(3/2)} - \frac{1}{400}\delta W_2^{(3/2)}$$
$$-\frac{1}{400}\delta W_1^{(5/2)} + \frac{1}{350}\delta W_2^{(5/2)} - \frac{1}{1120}\delta W_3^{(5/2)}. \tag{6}$$

Since each of the constants C is proportional to the same octupole moment, knowing the hyperfine splitting inside each of the fine-structure manifolds provides direct access to Ω.

III. ELECTRONIC-STRUCTURE FACTORS

Provided that the measurements of the HFS intervals are carried out, one could extract the octupole moment by computing the matrix elements of the electronic coupling tensor T_3^e. Specifically,

$$C(\gamma J) = -\Omega \begin{pmatrix} J & 3 & J \\ -J & 0 & J \end{pmatrix} \langle \gamma J || T_3^e || \gamma J \rangle.$$

We may also compute the second-order M1-E2 HFS correction ζ by computing the off-diagonal matrix elements of the electronic coupling tensors T_1^e and T_2^e. For $I = 3/2$, ζ is given by

$$\zeta = \frac{20}{\sqrt{3}} \frac{\mu Q \langle 5D_{3/2} || T_1^e || 5D_{5/2} \rangle \langle 5D_{5/2} || T_2^e || 5D_{3/2} \rangle}{E_{5D_{5/2}} - E_{5D_{3/2}}}.$$

Matrix elements of the electronic tensors are given in Ref. [14].

To calculate the electronic-structure factors for the HFS constants $C(5D_{3/2})$ and $C(5D_{5/2})$ and for the second-order term ζ we employ the correlation potential method [16] using all-order correlation correction operator $\hat{\Sigma}^{(\infty)}$ as suggested in Refs. [17, 18]. The method was used for Ba$^+$ previously [19] for accurate calculation of the parity non-conservation. It is also known that the method produces accurate results for the magnetic dipole hyperfine structure constants of alkali atoms (see, e.g. Ref. [20]).

Calculations start from the Hartree-Fock procedure for the closed-shell Ba^{2+} ion

$$(\hat{H}_0 - \epsilon_c)\psi_c = 0, \tag{7}$$

where $\hat{H}_0$ is the single-electron relativistic Hartree-Fock (RHF) Hamiltonian

$$\hat{H}_0 = c\alpha \cdot \hat{\mathbf{p}} + (\beta - 1)mc^2 - Ze^2/r + \hat{V}_{core}, \tag{8}$$

index c in Eq.(7) numerates core states, and $\hat{V}_{core}$ is the sum of the direct and exchange self-consistent potential created by $Z - 2$ core electrons.

States of the external electron are calculated using the equation

$$(\hat{H}_0 + \hat{\Sigma} - \epsilon_v)\psi_v = 0, \tag{9}$$

which differ from the equation for the core (7) by an extra operator $\hat{\Sigma}$. The so-called correlation operator $\hat{\Sigma}$ is defined in such a way that in the lowest order the correlation

6

correction to the energy of the external electron is given as an expectation value of the $\hat{\Sigma}$ operator

$$\delta\epsilon_v = \langle\psi_v|\hat{\Sigma}|\psi_v\rangle. \tag{10}$$

The correlation potential $\hat{\Sigma}$ is a non-local operator which is treated in the Hartree-Fock-like equations (9) the same way as a non-local exchange potential. Solving these equations we get the energies and the orbitals which include correlations. These orbitals are usually called *Brueckner orbitals*.

We use the Feynman diagram technique [17] and B-spline basis set [21] to calculate $\hat{\Sigma}$. The many-body perturbation theory (MBPT) expansion for $\hat{\Sigma}$ starts from the second-order and has the corresponding notation $\hat{\Sigma}^{(2)}$. However, we also include two dominating classes of the higher-order diagrams into the calculation of $\hat{\Sigma}$, as described in Ref. [17]. These higher-order effects are: (1) screening of Coulomb interaction between core and valence electrons by other core electrons and (2) an interaction between an electron excited from atomic core and the hole in the core created by this excitation. Both these effects are included in all orders and corresponding $\hat{\Sigma}$ is called $\hat{\Sigma}^{(\infty)}$. Another class of higher-order correlations is included in all orders when the equations (9) are iterated for the valence states. These higher-order effects are proportional to $\langle\hat{\Sigma}\rangle^2$, $\langle\hat{\Sigma}\rangle^3$, etc.

The effect of the second- and higher-order correlations on the energies of Ba$^+$ is illustrated by the data in Table I. As one can see, the inclusion of the correlations leads to systematic improvement in the accuracy for the energies. Note that since solving the equations (9) for Brueckner orbitals produces not only the energies but also the wave functions of the external electron, the better accuracy for the energy should translate into better accuracy for the wave function and for the matrix elements. Therefore, we can try to improve the wave function even further by fitting the energies to the experimental values by rescaling the $\hat{\Sigma}$ operator in Eq. (9). This is done by replacing $\hat{\Sigma}$ by $f\hat{\Sigma}$, where rescaling parameter f is chosen to fit experimental energies. The values of f for different states of Ba$^+$ are listed in Table I.

To calculate the HFS constants we need to include extra fields which are the fields of the nuclear P-even electromagnetic moments such as magnetic dipole, electric quadrupole, etc. This is done in the self-consistent way similar to the RHF calculations for the energies in the frameworks of the well-known random-phase approximation (RPA). Corresponding

TABLE I: Removal energies of Ba^+ in different approximations [cm^{-1}].

State	J	RHF	$\Sigma^{(2)}$	$\Sigma^{(\infty)}$	fitted[a]	Expt.[b]
$6S$	1/2	75339	82227	80812	80685	80687
$6P$	1/2	57265	61129	60584	60442	60425
$6P$	3/2	55873	59351	58863	58735	58734
$5D$	3/2	68138	77123	76380	75816	75813
$5D$	5/2	67664	76186	75543	75004	75012

[a] $f(6s)=0.978$, $f(6p)=0.960$, $f(5d)=0.934$
[b] NIST, Ref. [22]

equations have the form

$$(\hat{H}_0 - \epsilon_c)\delta\psi_c = -(\hat{F} + \delta\hat{V}_{core})\psi_c, \tag{11}$$

where $\hat{F}$ is the operator of external field, $\delta\psi_c$ is the correction to the core state due to the effect of external field and $\delta\hat{V}_{core}$ is the correction to the self-consistent Hartree-Fock potential due to the change in field-perturbed core states. The RPA equations (11) can be considered as a linearized (in external field) expansion of the RHF equations (7); these are also solved self-consistently for all the core states. This corresponds to the inclusion of the so-called *core polarization* (CP) effect. Matrix elements for states of the external electron are given by

$$\langle\psi_v|\hat{F} + \delta\hat{V}_{core}|\psi_v\rangle. \tag{12}$$

Dominant correlations are included by simply using the Brueckner orbitals as the wave functions ψ_v in (12). There are, however, correlation corrections to the matrix elements which are not included into (12). These are the *structure radiation* (SR) and the effect of normalization of the many-electron wave function [16]. Structure radiation can be described as a contribution due to the change in $\hat{\Sigma}$ caused by the effect of the external field:

$$\langle\psi_v|\delta\hat{\Sigma}|\psi_v\rangle. \tag{13}$$

We calculate SR and renormalization contributions using the MBPT similar to the third-order calculations presented in Ref. [23] (second-order in Coulomb interaction and first-order in external field). However, we use the "dressed" operators of the external field: $\hat{F} + \delta\hat{V}_{core}$ rather than just $\hat{F}$ as in Ref. [23]. Therefore, core polarization effect is included in all orders

in the SR and renormalization calculations. We also use two different basis sets of single-electron states. One is the dual kinetic-balance basis (DKB) set [24, 25], and another is the B-spline basis set developed at the University of Notre Dame [21].

The results of the calculations are presented in Table II. Here the RHF approximation corresponds to the $\langle \psi_v^{\mathrm{HF}} | \hat{F} | \psi_v^{\mathrm{HF}} \rangle$ matrix elements with the Hartree-Fock orbitals ψ_v^{HF}. RPA approximation corresponds to the $\langle \psi_v^{\mathrm{HF}} | \hat{F} + \delta \hat{V}_{core} | \psi_v^{\mathrm{HF}} \rangle$ matrix elements. Brueckner + CP approximation corresponds to the $\langle \psi_v^{\mathrm{Br}} | \hat{F} + \delta \hat{V}_{core} | \psi_v^{\mathrm{Br}} \rangle$ matrix elements with Brueckner orbitals ψ_v^{Br}, etc. The values of the SR and renormalization corrections listed in Table II were computed with the DKB basis set.

TABLE II: Magnetic octupole hyperfine structure constant C of the $5D_{3/2}$ and $5D_{5/2}$ states of Ba$^+$ and off-diagonal matrix elements of the magnetic dipole and electric quadrupole operators in different approximations.

Approximation	$C(5D_{3/2})$	$C(5D_{5/2})$	$\langle 5D_{3/2}||T_1^{(e)}||5D_{5/2}\rangle$	$\langle 5D_{5/2}||T_2^{(e)}||5D_{3/2}\rangle$
	kHz/ $(\Omega/(\mu_{\mathrm{N}} \times \mathrm{b}))$	kHz/ $(\Omega/(\mu_{\mathrm{N}} \times \mathrm{b}))$	MHz/μ_N	MHz/b
RHF	-0.4294	-0.1514	-95	180
RPA $\equiv$ RHF + CP	-0.5843	0.9636	-1360	184
$\Sigma^{(2)}$ + CP	-0.6863	0.9254	-1496	222
$\Sigma^{(\infty)}$ + CP	-0.6822	0.9244	-1489	220
Energy fitting (Br)	-0.6758	0.9282	-1481	218
SR	0.0842	-0.8472	280	14
Norm	0.0178	-0.0287	42	-5
Total (Br+SR+Norm)	-0.5738	0.0523	-1160	227

IV.   EXTRACTING OCTUPOLE MOMENT

Our final results for the magnetic octupole hyperfine structure constants are

$$C(5D_{3/2}) = -0.585(11) \left(\frac{\Omega}{\mu_N \times \mathrm{b}} \right) \mathrm{kHz},$$
$$C(5D_{5/2}) = 0.036(16) \left(\frac{\Omega}{\mu_N \times \mathrm{b}} \right) \mathrm{kHz}. \tag{14}$$

Here central values and the errors are found from the scattering of the results due to effects of energy fitting and change of basis for the SR and renormalization calculations. Notice that the error bars are purely theoretical and reflect the fact that only certain classes of diagrams are included in the calculations. In particular, there are strong cancelations between various contributions to the $C(5D_{5/2})$ constant, leading to a large, 45%, uncertainty in the value of this constant.

The above error estimates are consistent with the general trend for the experimentally known constants A and B of the $5D_J$ states [26]. Our employed method is off by as much as 10% for $A(5D_{3/2})$ and 30% for $A(5D_{5/2})$. The computed values of B generally agree at the level of a few per cent with the experiment. Another insight comes from understanding that the theoretical method includes the RPA and Brueckner chains to "all orders"; as long as these classes of diagrams dominate, the theoretical accuracy is excellent. By contrast, in case of the $C(5D_{5/2})$ the result is accumulated due to remaining SR and Norm diagrams (see Table II), which are computed nominally in the third-order MBPT only. This explains the relatively poor accuracy for the $5D_{5/2}$ states. As demonstrated in Ref. [27] (at least for the constants A and B) the theoretical accuracy could be improved to 1% by employing the relativistic coupled-cluster method.

The results, Eqs. (14), may be used to extract the values of the nuclear magnetic octupole moment from the measurements. For example, if equation (6) is used then

$$C(5D_{3/2}) + \frac{1}{10}C(5D_{5/2}) = -0.581(13) \left(\frac{\Omega}{\mu_N \times \text{b}}\right) \text{ kHz.} \tag{15}$$

Alternatively, one can use the first equation of (5). Then the correction due to the second-order term ζ needs to be taken into account. With the values of the magnetic dipole and electric quadrupole HFS matrix elements presented in the last columns of Table II this correction reads

$$\Delta C(5D_{3/2}) = -\frac{1}{2000\sqrt{21}}\zeta = \begin{cases} 1.84 \text{ Hz } ^{135}\text{Ba}^+ \\ 3.17 \text{ Hz } ^{137}\text{Ba}^+ \end{cases} \tag{16}$$

Notice that in this second scenario we advocate using the $5D_{3/2}$ hyperfine manifold for extracting the nuclear octupole moment because of the poor theoretical accuracy of computing electronic couplings for the $5D_{5/2}$ state.

We may evaluate the relative influence of Ω on the HFS by using the single-particle

(shell-model) estimate for the nuclear octupole moment, Eq. (2); we arrive at

$$C(5D_{3/2})^{\text{s.p.}} \approx -23 \,\text{Hz}\,,$$

$$C(5D_{5/2})^{\text{s.p.}} \approx 1.4 \,\text{Hz}\,.$$

We see that the second-order correction, $\Delta C(5D_{3/2})$, is below the anticipated value of the constant.

At this point we briefly discuss the effect of all other second- and higher-order terms past η and ζ, which until this point have been assumed negligible. One might expect other second-order dipole-dipole terms which mix in states outside of the $5D$ fine structure manifold to have an appreciable effect on the hyperfine structure. However, the proof in Ref. [14] can easily be generalized to show that *no* second-order dipole-dipole terms enter into the equations for the C constants, Eqs. (5). Furthermore, it is found that the leading third-order term, the dipole-dipole-dipole term mixing the fine structure levels, drops out of Eq. (6) along with ζ. Therefore, we can expect the largest terms neglected from Eq. (6) to be the second-order dipole-octupole and quadrupole-quadrupole terms; we have estimated these effects to both be at the $\sim 10^{-3}$ Hz level. This provides sufficient confirmation that all second- and higher-order terms may be neglected in our proposed scheme of extracting the octupole moment.

Finally, using the single-particle approximation for the nuclear octupole moment, we obtain an estimated value for the left hand side of Eq. (6) of -22 Hz. Assuming a conservative value of 1 Hz uncertainty in the $5D$ HFS intervals yields an overall uncertainty of 0.017 Hz in the right hand side of Eq. (6). In the next section we describe how such measurements should be capable of much smaller uncertainties, 0.1 Hz or better. Thus we may conclude that HFS interval measurements with readily attainable accuracy, combined with the theoretical result (15), would be capable of extracting an octupole moment of the estimated size for the ^{135}Ba and ^{137}Ba nuclei.

V.   EXPERIMENTAL POSSIBILITIES

The measurements can be carried out by a technique similar to one already used to study transitions among sublevels of the $5D_{3/2}$ state of Ba$^+$ [15], in which optical pumping is used to place the ion in a particular sublevel, and an RF transition to another sublevel is
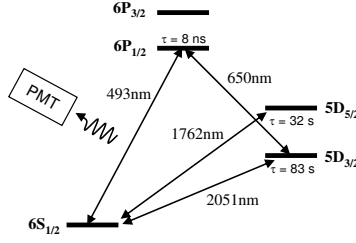
FIG. 1: The lowest S, P, and D states of Ba^+, showing the cooling 493 nm and cleanup 650 nm transitions plus the 2051 nm and 1762 nm E2 transitions to the metastable D states.
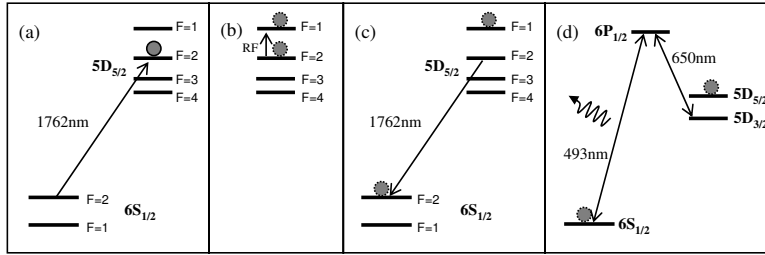

FIG. 2: Procedure for measuring the hyperfine intervals in the $5D_{5/2}$ state. (a) First, a 1762 nm resonant laser pulse transfers the ion into the $F = 2$ hyperfine sublevel of the $5D_{5/2}$ state. (b) The RF is then applied to drive a hyperfine transition in the $5D_{5/2}$ state. (c) The second pulse of the 1762 nm laser depopulates the $5D_{5/2}$ $F = 2$ level. (d) To determine if the hyperfine transition in the $5D_{5/2}$ state occurred, the cooling and the cleanup lasers are turned on and any ion fluorescence is detected. Absence of fluorescence indicates that the RF is on resonance and caused the transition to take place.

detected by the effect of "shelving" as described below. Such measurements are performed on a single ion held by radio frequency electric fields in a 3-dimensional effective potential well typically $\approx 100\text{eV}$ deep, with the ion at the bottom of the well after being laser cooled to a temperature $\cong 10^{-3}\deg\text{K}$, with an orbital diameter $\cong 10^{-2}\mu\text{m}$.

The electronic energies of the lowest S, P, and D states of Ba^+ are shown in Fig. 1. The cooling laser operates on the $6S_{1/2} - 6P_{1/2}$ allowed $E1$ absorption line near 493 nm, mistuned slightly to the red of resonance to effect Doppler cooling. A 'cleanup' laser beam operates at the $6P_{1/2} - 5D_{3/2}$ transition near 650 nm to keep the ion from getting stuck in the metastable D state and lost to the cooling process.

To measure the hyperfine splitting of either $5D$ state, the ion can be initially placed in the ($F_g = 2$, $M_F = 0$) Zeeman sublevel of the $6S_{1/2}$ ground state by optical pumping with a polarized 493 nm beam. As shown in Fig. 2, in the case of the $5D_{5/2}$ measurement the ion is then transferred to a particular hyperfine sublevel (F, M_F) of $5D_{5/2}$ by applying a pulse of resonant 1762 nm light. RF field coils are then turned on for driving a $\Delta F = \pm 1$ transition, after which a second pulse of the 1762 nm laser will transfer from (F, M_F) back to the ground state. The ion therefore ends up in the ground state if there was no hyperfine transition, and in $5D_{5/2}$ if the RF is on resonance and the hyperfine transition was successful. In the former case there will be fluorescence when the ion is illuminated by the 493 nm/650 nm lasers while in the latter case there will not be fluorescence; the ion is 'shelved' in the $5D_{5/2}$ state. The process is repeated for a range of RF frequencies and a hyperfine transition resonance curve is acquired. For the $5D_{3/2}$ measurement, the same procedure is followed with 2051 nm resonant light to populate $5D_{3/2}$ sublevels, but an extra step is needed at the end – the shelving of the $6S_{1/2}$ state population to the $5D_{5/2}$ state.

TABLE III: Zeeman splitting coefficients defined in Eq. (18).

M_F	a_1 (MHz/G)	a_2 (MHz/G)	a_3 (MHz^2/G^2)
3	3.359	0.2099	0.7052
2	2.239	0.1400	1.153
1	1.120	0.06998	1.422
0	0	0	1.511
−1	-1.120	-0.06998	1.422
−2	-2.239	-0.1400	1.153
−3	-3.359	-0.2099	0.7052

In the previous measurements of Zeeman transitions among $5D_{3/2}$ sublevels, sensitivities of a few Hz were achieved [15], limited by incompletely shielded magnetic field fluctuations. In the hyperfine measurements proposed here, this source of broadening can be eliminated by using transitions that have a weak magnetic field dependence, such as $M_F = 0 \rightarrow M_F = 0$. In practice, it is often easiest to perform laser cooling in nonzero magnetic fields (typically $B \cong 1$G) to avoid formation of inefficiently cooled dark states. Such modest magnetic fields will introduce only a small B^2 dependence in the $0 \rightarrow 0$ transition when the energy

separations between hyperfine levels are sufficiently large. In fact the Zeeman effect for $B = 1G$ can indeed be considered a small perturbation to the hyperfine splitting for all the $5D_{3/2}$ states and for the $F = 1$ and $F = 2$ states of the $5D_{5/2}$ manifold.

However, for the $5D_{5/2}$ $F = 3$ and $F = 4$ states the situation is more complicated because the hyperfine splitting between these states is small, $\cong 0.49$ MHz [26], so the Zeeman Hamiltonian cannot be considered a weak perturbation to the hyperfine Hamiltonian. The Zeeman and hyperfine Hamiltonians must therefore be treated on an equal footing. The manifold of $F = 3$ and $F = 4$ states are then all degenerate in zeroth order, and the first-order energy shifts due to $H_{Zeeman} + H_{hyp}$ are obtained by diagonalizing the matrix of $H_{Zeeman} + H_{hyp}$ within the manifold of $F = 3$ and $F = 4$. In the $|IJFM_F\rangle$ basis, the matrix is 2x2 block diagonal, with each block having a given value of M_F. The eigenvalues are then given by

$$E_{\pm} = \frac{1}{2}E_3 + a_1 B \pm \sqrt{\frac{1}{4}E_3^2 + a_2 E_3 B + a_3 B^2} \tag{17}$$

where E_+ reduces to the $F = 3$ hyperfine energy E_3 for $B = 0$ and E_- reduces to the $F = 4$ hyperfine energy, which is here taken as zero. The values of a_1, a_2, and a_3 are given in Table III. These are related to the matrix elements of the Zeeman Hamiltonian H' as follows

$$a_1 B = \frac{1}{2} \left(\langle 4, M_F | H' | 4, M_F \rangle + \langle 3, M_F | H' | 3, M_F \rangle \right),$$

$$a_2 B = -\frac{1}{2} \left(\langle 4, M_F | H' | 4, M_F \rangle - \langle 3, M_F | H' | 3, M_F \rangle \right),$$

$$a_3 B^2 = \frac{1}{4} \left(\langle 4, M_F | H' | 4, M_F \rangle - \langle 3, M_F | H' | 3, M_F \rangle \right)^2 + \left(\langle 4, M_F | H' | 3, M_F \rangle \right)^2. \tag{18}$$

A portion of the graph of the energy levels as a function of B is given in Fig. 3. Note that for even small magnetic fields there is a great deal of mixing between the $F = 3$ and $F = 4$ states, and there are two energy levels, originating from $F = 3$, $M_F = -1$ and $F = 4$, $M_F = 1$, that are almost field-independent for B in the range of $\simeq 0.6G - 1.2G$. Each of these levels can be connected to the $F = 2$, $M_F = 0$ level by an RF transition, with very weak dependence on B. Likewise, the desired zero-field hyperfine intervals can be extracted from these RF measurements using only a relatively low resolution determination of B by a field-dependent Zeeman resonance. Thus measurement of all hyperfine intervals to 0.1 Hz seems feasible.

We have shown that a simultaneous measurement of the hyperfine splittings in the $5D_{3/2}$ and the $5D_{5/2}$ fine structure levels of Ba^+ allows one to unambiguously extract the value
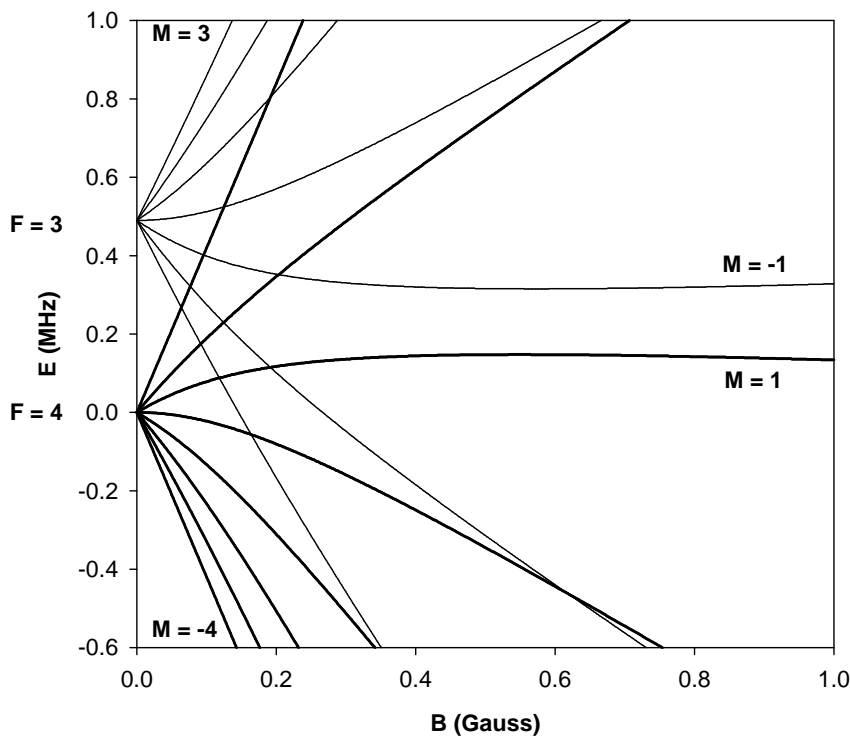
FIG. 3: $D_{5/2}$ $F = 3$ and $F = 4$ hyperfine Zeeman levels. Energies are measured relative to the $F = 4$ energy at zero magnetic field. Very small mixing of the $F = 3$ state with the $F = 2$ state has been neglected.

for the nuclear magnetic octupole moment. We performed the *ab initio* calculations of the relevant matrix elements in the framework of relativistic many-body perturbation theory, analyzing the first- and the second-order corrections to the hyperfine energy levels. We have also outlined an experimental procedure for measuring the hyperfine intervals to the required accuracy with single trapped Ba$^+$ ions.

Acknowledgments

---

[1] C. Schwartz, Phys. Rev. **97**, 380 (1955).

[2] R. A. Senkov and V. F. Dmitriev, Nucl. Phys. A **706**, 351 (2002).

[3] V. F. Dmitriev, private communication.

[4] V. Gerginov, A. Derevianko, and C. E. Tanner, Phys. Rev. Lett. **91**, 072501 (2003).

[5] C. Schwartz, Phys. Rev. **105**, 173 (1957).

[6] R. T. Daly and J. H. Holloway, Phys. Rev. **96**, 539 (1954).

[7] H. H. Brown and J. G. King, Phys. Rev. **142**, 53 (1966).

[8] T. G. Eck and P. Kusch, Phys. Rev. **106**, 958 (1957).

[9] W. J. Childs, O. Poulsen, L. S. Goodman, and H. Crosswhite, Phys. Rev. A **19**, 168 (1979).

[10] W. J. Childs, Phys. Rev. A **44**, 1523 (1993).

[11] T. Brenner, S. Buttgenbach, W. Rupprecht, and F. Traber, Nucl. Phys. A **440**, 407 (1985).

[12] W. G. Jin, M. Wakasugi, T. T. Inamura, , T. Murayama, T. Wakui, H. Katsuragawa, T. Ariga, T. Ishizuka, and I. Sugai, Phys. Rev. A **52**, 157 (1995).

[13] D. A. Landman and A. Lurio, Phys. Rev. A **1**, 1330 (1970).

[14] K. Beloy, A. Derevianko, and W. R. Johnson, Phys. Rev. A **77**, 012512 (2008).

[15] J. A. Sherman, T. W. Koerber, A. Markhotok, W. Nagourney, and E. N. Fortson, Phys. Rev. Lett. **94**, 243001 (2005).

[16] V. A. Dzuba, V. V. Flambaum, P. G. Silvestrov, and O. P. Sushkov, J. Phys. B **20**, 1399 (1987).

[17] V. A. Dzuba, V. V. Flambaum, and O. P. Sushkov, Phys. Lett. A **141**, 147 (1989).

[18] V. A. Dzuba, V. V. Flambaum, A. Y. Kraftmakher, and O. P. Sushkov, Phys. Lett. A **142**, 373 (1989).

[19] V. A. Dzuba, V. V. Flambaum, and J. S. M. Ginges, Phys. Rev. A **63**, 062101 (2001).

[20] V. A. Dzuba and V. V. Flambaum, Phys. Rev. A **62**, 052101 (2000).

[21] W. R. Johnson, S. A. Blundell, and J. Sapirstein, Phys. Rev. A **37**, 307 (1988).

[22] Y. Ralchenko, A. E. Kramida, J. Reader, and NIST ASD Team, *NIST atomic spectra database (version 3.1.4)* (2008), URL `http://physics.nist.gov/asd3`.

[23] W. R. Johnson, Z. W. Liu, and J. Sapirstein, At. Data Nucl. Data Tables **64**, 279 (1996).

[24] V. M. Shabaev, I. I. Tupitsyn, V. A. Yerokhin, G. Plunien, and G. Soff, Phys. Rev. Lett. **93**, 130405 (2004).

[25] K. Beloy and A. Derevianko, *Application of the dual-kinetic-balance sets in the relativistic many-body problem of atomic structure* (2007), arXiv:0710.3142.

[26] R. E. Silverans, G. Borghs, P. De Bisschop, and M. Van Hove, Phys. Rev. A **33**, 2117 (1986).

[27] B. K. Sahoo, Phys. Rev. A **74**, 020501 (pages 4) (2006).